Arab J Geosci (2013) 6:1191–1202
DOI 10.1007/s12517-011-0411-7

ORIGINAL PAPER

# Assessing flash flood hazard in an arid mountainous region

**Eman Ghoneim · Giles M. Foody**

Received: 30 June 2011 / Accepted: 18 September 2011 / Published online: 29 September 2011


**Abstract** Although flash floods are one of the major natural disasters that may hamper human development in arid areas, aspects of the process leading to their initiation remain uncertain and poorly understood. In the present study, wadi El-Alam Basin, one of the major basins in the Eastern Desert of Egypt that is frequently subjected to severe flash flood damage, is selected for investigation. Here, a hydrological modeling approach was used to predict flash flood hazard within the basin. Earlier work conducted for the same basin showed that such approach is successful and was able to accurately highlight the locations of historical flood damage. However, such work was based on one set of arbitrary model parameters. The present study has taking into account the rainfall as the excitation factor in the adopted hydrological modeling. The study aims to build on the earlier study by investigating impacts of variation of rainfall depth, areal coverage, and location on flash flood generation. Results demonstrate that the basin under study requires a rainstorm intensity of at least 40 mm in order to initiate surface runoff with a noticeable flood peak at its main outlet. The location of rainstorm has a major effect on the shape of the basin final hydrograph. Furthermore, in the study basin, the upstream flood appears to be of a magnitude and a peak flow that is much higher than those for downstream ones, which believes to be strongly attributed to the surface steepness and impermeability of the former. The used approach shows to be useful in the rapid assessing of flash flood hazard in mountainous desert and could be adopted, with appropriate modifications, elsewhere in arid regions.

**Keywords** GIS · Digital elevation model · Remote sensing · Hydrologic modeling · Wadi Alam · Eastern Desert · Egypt

E. Ghoneim (✉)
Department of Geography and Geology,
University of North Carolina Wilmington,
601 South College Road,
Wilmington, NC 28403-5944, USA
e-mail: ghoneime@uncw.edu

G. M. Foody
School of Geography, University of Nottingham,
University Park,
Nottingham NG7 2RD, UK

## Introduction

Flash flooding in arid regions is a double-edged natural phenomenon, being simultaneously a blessing and a curse. It is a blessing as the flood water is a major source of groundwater recharge in arid regions. It is also, however, a curse as the tremendous power of the water flow is able to cause devastation along its pathway.

A flash flood is a hydrometeorological event and is distinguished from “ordinary” floods by the time scale of the event. Whereas floods may occur over periods of several days or more and it may be possible to attempt damage mitigation actions (like sandbagging), flash floods occur much too rapidly for such preparations. Flash flood events in arid regions can develop in periods of hours or less, which makes them particularly dangerous to human health and well-being. These arid areas experience occasional very intense and often short-duration rainstorm events (Greenbaum et al. 1998) that create flash floods that can run rapidly along dense network of mountainous wadis that drain the mountains. These rainstorm events frequently cause severe flooding and damage human infrastructure.

Recent studies on the damage caused by desert flash floods have highlighted the role played by the humans in exaggerating the destructive effects of these events (Grodek et al. 2000). Many towns in deserts and their associated networks of roads intercept, in some way or the other, the flow of the floods. Therefore, in any flood risk assessment study, one has to be concerned not only with the flood itself as hazardous source but also with its receptors (the target elements, mostly human constructions) and pathways (the channel networks, which transport the hazard of the flood to the targets). The combination of these three factors determines the magnitude of the flood risk.

While flash flooding has been recognized as an environmental hazard for many decades, aspects of the processes leading to its initiation and controlling its attributes (e.g., severity) remain uncertain or, at least, less than adequately documented (Schick et al. 1997). Due to the very long intervals between flood events, relatively little attention has sometimes been paid to these natural processes, resulting in the local population having a fallacious sense of security from destructive flash floods. Moreover, newcomers to sensitive regions often settle and develop the land without consideration of the potential flood hazard. The extremely arid climate and long series of floodless years may encourage the locals to downplay the flood damage shortly after its occurrence, leading to an overall neglect in the maintenance of drainage ways (channel network), which may have been inactive for years (Grodek et al. 2000). As a result of these and other issues, the ability to understand the flooding process and use this knowledge to minimize its threat to human health and well-being is limited.

The ability to accurately predict sites vulnerable to flash flooding would help in planning measures to protect such sites from future damage and help in planning new developments such as roads and housing. To locate sites vulnerable to flood risk, it is important to identify the hydrological properties of such sites. Typically these properties could be derived from the surface topology of the terrain (Patton and Baker 1976; Costa 1987; Patton 1988) and land cover characteristics (Gheith and Sultan 2002). Key surface topology variables such as slope and flow path can be derived from digital elevation model (DEM), while land cover characteristics, such as water loss by infiltration, can be inferred from satellite sensor images. Consequently, surface topology and land cover maps can be used to parameterize hydrological models (Gheith and Sultan 2002; Hammouri and El-Naqa 2007) to predict flood risk (Foody et al. 2004). In particular, a hydrological model can be used to predict the shape and magnitude of the storm hydrograph that may help in identifying sites vulnerable to flash flood risk. The ultimate objective of this study is to explore the hydrological response of the study basin to a rainfall event and how this could be used to assess the flood response in the town of Marsa Alam and along the major highway of Idfu-Alam that crosses the basin.

## Study area

The basin under study, wadi El-Alam, lies in the Egyptian Eastern desert (Fig. 1). It runs from the high rugged mountains in the west toward the Red Sea coast in the east with a total drainage area of 407 $km^2$. A major urban area, Marsa Alam, is located on the delta of the wadi El-Alam and connected west to the town of Idfu on the Nile River by a highway (termed Idfu-Alam road) that runs through the dry riverbed (Fig. 2). Consequently, both the town and the road are at danger from flash flood hazards (Fig. 3a).

The basin itself is ungauged and there is little detailed metrological and hydrological data for it. Although located within an arid region, with an average annual rainfall of 13 mm, the area does experience infrequently intense rainstorms. Such rainstorms can rapidly generate flash floods because of their intensity, which have reached up to 60 mm $h^{-1}$ at nearby locations (Gheith and Sultan 2002).

The wadi banks are bounded by high rocky hills that reduce its channel width from 1,200 to less than 100 m (Fig. 3b). Such narrowing in channel course causes a frequent concentration of floodwaters and hence increases the destructive effect of the flow during rainy storms. In spite of this situation, the urban area of Marsa Alam continues to grow outward over its hazardous dry river bed. Recent development has taken place on top of the surrounding rocky hills in order to avoid damaging by flood water. However, they seem to be still prone to flood risk due to lateral erosion causing by flood water during heavy rainstorm events (Fig. 3c). Wadi El-Alam contains also sections of the Red Sea coastal highway and the Idfu-Alam highway, which both are subjected to flash flood risk. The crossing of the latter highway to a series of alluvial fans gives rise to many problems, such as erosion and deposition by large amount of sediments which eventually impede traffic use of such highway.

## Data and methods

In the absence of sufficient data on surface flow for the study basin, the only feasible means of predicting the dynamics of surface runoff and water loss was to adopt a modeling approach supported by acquisition of data on surface elevation properties, land cover, and associated hydrological variables. Here the watershed-oriented hydrological modeling system (HMS) (Peters 1998), developed by the Hydrologic Engineering Center (HEC) of the US

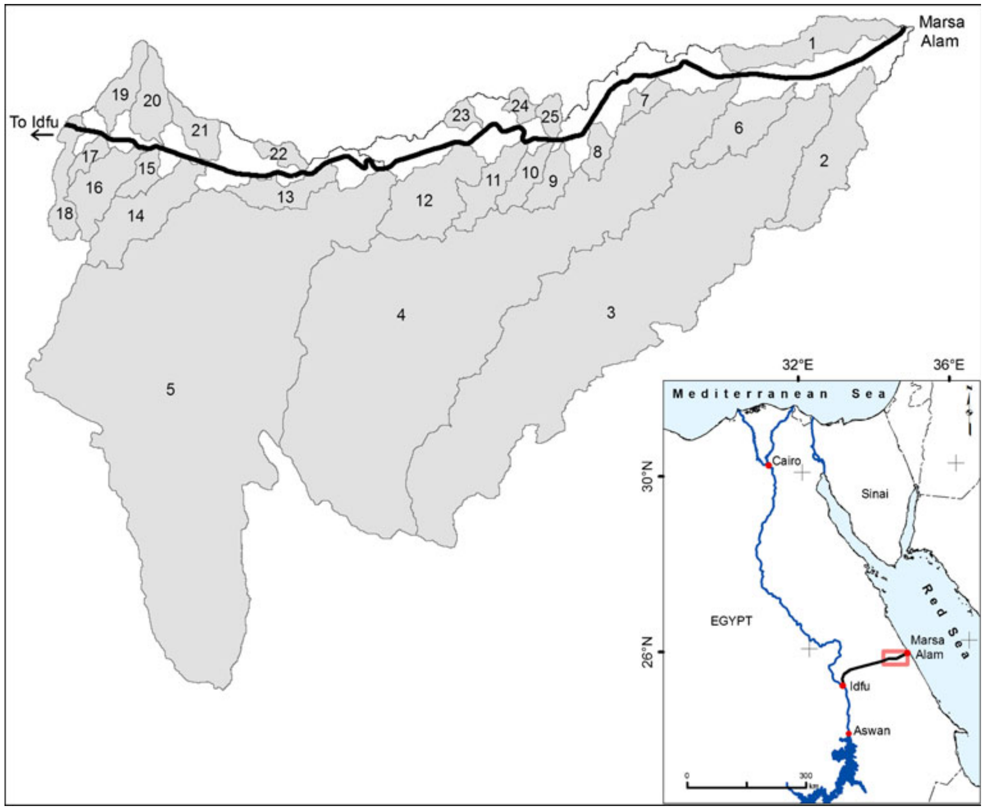


**Fig. 1** The drainage basin of Wadi El-Alam. *Lower right*, the location map of the study site

Army Corps of Engineers, has been utilized to model the rainfall–runoff process and to predict basin behaviors through the construction of hydrographs. The used model requires surface topography and water loss as parameters for generating basin flow responses. The former was generated from the DEM, while the latter was derived by satellite remote sensing. Validation for the HEC-HMS in number of watersheds in arid regions, which are similar in hydrologic properties to the study basin, was performed and the results were satisfactory (e.g., Al-Abed et al. 2005; Hammouri and El-Naqa 2007).

DEM of the area (Fig. 4a) was derived from topographic contours that were digitized manually from 1:50,000 scale topographic maps of the site using the ARCGIS v. 9.3.1 software. To identify the sites prone to flooding along the Idfu-Alam road, the direction and accumulation of the basin flow were calculated. For this, the D8 flow algorithm (Jenson and Domingue 1988), which is widely used in the literature (e.g., Ghoneim and El-Baz 2007; Ghoneim et al. 2007), has been employed for generating the surface flow directions. By making use of these flow data, the channel network of the basin was defined and the crossing points (outlets) of this network with the Idfu-Alam highway were located. With the aid of the geographic information system, sub-basins areas that drain to each of these crossing points were highlighted. A total of 55 sub-basins were delineated. After the exclusion of sub-basins of areas less than 1 km$^2$ (assumed to be too small to have a pronounced flood damage effect), 25 sub-basins remained.

The water losses due to infiltration were computed using the Soil Conservation Service Curve Number (CN) method (SCS 1985). This method has been used in calculating water loss in arid and semi-arid regions (e.g., Sorman et al. 1990; Gheith and Sultan 2002; Hammouri and El-Naqa 2007; Ghoneim 2008). The CN is a function of soil and land cover conditions and can be estimated using published tables (SCS 1985) from information on antecedent moisture conditions, land cover, and soil type. The estimation of the CN, therefore, required information on these three variables. For this test site, in an arid environment, it seems reasonable to assume dry antecedent moisture conditions (Gheith and Sultan 2002).

The land cover information required for the hydrological modeling were derived with the aid of a supervised digital image classification (Tso and Mather 2001) of Landsat ETM+ imagery (acquired on March 2003) of the site (Fig. 4b). Image pre-processing, using ENVI v. 4.8 software, involved geometric, atmospheric, radiometric, and topographic correction of the remotely sensed data. The supervised classification (using the maximum likelihood method) aimed to obtain a thematic layer from the imagery in which the land cover classes mapped varied in terms of their hydrological characteristics. The resulted land cover map found to contain five main classes, which are

**Fig. 2** **a** Field photos of the upper-stream area of the El-Alam drainage basin. **b** Field photo of the town of Marsa Alam with the Red Sea coast shown at the background

basement outcrop, sedimentary rocks, desert pavement, and consolidated and unconsolidated wadi bed deposits. The physical differences between these five classes most likely cause differences in their infiltration and runoff properties. The spatial distribution of these classes within a watershed would, consequently, impact significantly on the watershed's response to a rainfall event. Settlements and roads, which were manually digitized from 1:50,000 scale topographic maps (produced by Egyptian Military Survey) of the site, were added to the derived land cover map as an extra classes. The final seven-class land cover map (see Fig. 4b) was used in the estimation of the CN values in the HMS-based analyses.

A fieldwork has been conducted to evaluate the textural and infiltration properties of the non-rock classes (the desert pavement, the consolidated and unconsolidated wadi bed deposits, Fig. 5), which was required for the specification of the CN values in the model (SCS 1985). At a total of 16 sites, a soil sample of 500 g derived from the uppermost 50 cm of the soil was obtained for textural analysis. Each soil sample was sieved to separate the soil particles by size to enable specification of the relevant SCS soil group. The infiltration rate of each class was also assessed. Using a ring infiltrometer, inserted to a depth of 15 cm, the rate of infiltration was assessed with the change in measured vertical infiltration as a function of time used to derive an estimate of the infiltration rate (Philip 1957).

Together, the information on soil texture and infiltration were used to determine the soil group for each of the seven classes that were derived through image classification. Based on the SCS soil classification (SCS 1985), soils are categorized into one of four different types ranked from A to D on the basis of their runoff potential. Results shown that the surface deposits of the basin under study are belonging to two different soil groups A and D. Although the three non-rock soil classes (the desert pavement, the consolidated and unconsolidated wadi bed deposits) exhibited different textures, they did not differ significantly in terms of the SCS soil group classification. From the textural description derived, all three soils appeared to belong to soil group A, being coarse textured with little silt and clay and so having a low runoff potential. Field measurements of infiltration rate, however, show considerable differences between the three soil types, for example, ranged from 0.07 cm $h^{-1}$ on the desert pavement through 9.70 and 14.01 cm $h^{-1}$ for the consolidated and unconsol-

**Fig. 3** **a** Four field photos taken 2 h after a major rainstorm that occurred in 1996. They show a damaged sector of the coastal highway by the flood water (*left*, *top*, and *bottom*) and flood water in the downstream area of wadi El-Alam Basin (*right*, *top*, and *bottom*). **b** The narrow channel at the outlet of wadi El-Alam Basin. **c** Local residents using rocky boulders to strengthen the hillside of the dry river at the downstream area

idated wadi bed deposits, respectively (Foody et al. 2004). The remaining four classes of bedrock outcrops (sedimentary and basement), paved road network and residential areas, were all assigned to soil group D, which has the lowest infiltration capacity. Information about soil texture and infiltration, of the study area, are discussed in more details by the authors in Foody et al. (2004).

With the DEM and CN, derived from the soil and land cover data, and by adopting the Muskingum flow routing method (Chow et al. 1988), the HMS model was executed.

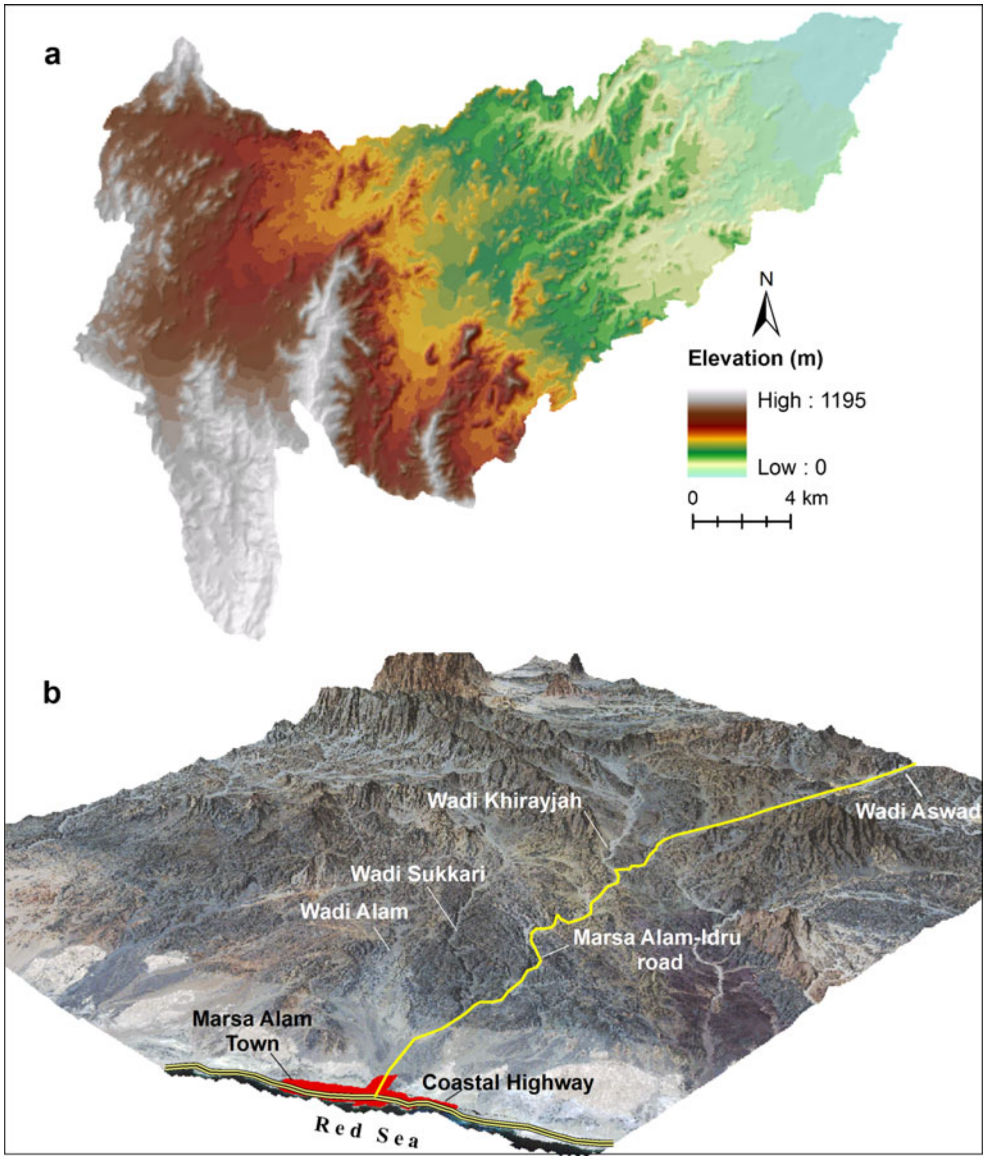


**Fig. 4** **a** DEM of the study basin. **b** An oblique, 3D perspective view of the study area, showing the location of Marsa Alam Town at the basin outlet. Sections of the Red Sea coastal highway and the Idfu-Alam highway are also visible in the figure

The stream velocity and Muskingham $X$ parameters were set at 3 m s$^{-1}$, typical of that observed in dry regions (Reid et al. 1998), and 0.2, respectively. These inputs were used to derive the average CN, channel slope, longest flow path, and lag time for each sub-watershed. The latter was computed from the SCS formula (Chow et al. 1988) as follows:

$$t_{\mathrm{lag}} = {L_{\mathrm{w}}}^{0.8} \times [1,000/\mathrm{CN}) - 9]^{0.7}/31.67S^{0.5} \qquad (1)$$

where $t_{\mathrm{lag}}$ (in minutes) is the sub-watershed lag time measured from the centroid of the hyetograph to the peak time of the hydrograph, $L_{\mathrm{w}}$ is the length of the longest flow path, $S$ (in percent) is the slope of the longest flow path, and CN is the average curve number of the sub-basin derived from the land cover and soil data.

In this study, a rainfall event with an intensity of 30 mm h$^{-1}$ over a period of 2 h was assumed. This value lies within the range of storms observed in the general region (e.g., Gheith and Sultan 2002) and was observed for the nearby Quseir station on 14 November 1996 (Egyptian Meteorological Authority, personal communication). It was also assumed that the rainstorm uniformly and exclusively covered a specified single basin on each run of the model and a time step of 30 min has been set. The output of the data processing was the calculation of the flood hydrographs for the outlet of wadi El-Alam Basin and each of its sub-watersheds. These hydrographs will describe potential for flood damage in the study basin.

As mentioned earlier, one of the main aims of this study is to identify sites prone to flash floods along the Idfu-Alam highway. Because the area of interest is arid, the hazard in such environments has to be relatively measured by the damage of any flood occurrences in the area. Undoubtedly, the damage of a flood is in direct relationship with its peak

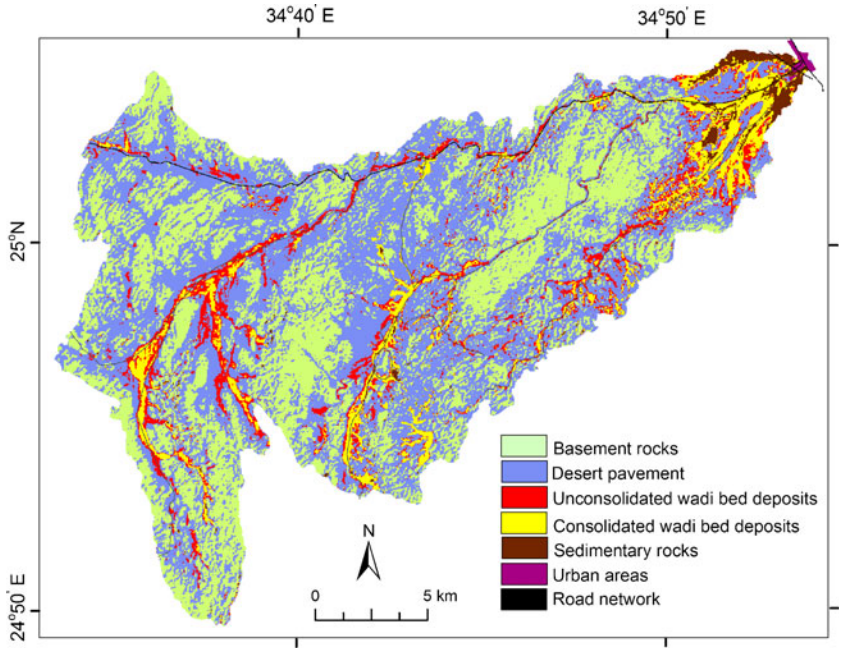


**Fig. 5** The land cover/use map of the basin, derived from a supervised classification of Landsat imagery

discharge not with its total amount of discharge. Accordingly, the peak discharge for each sub-basin that drains toward the highway was estimated by the HMS model. Under the assumption that basins of comparable physiographic characteristics will respond similarly to a given rainstorm, these sub-basins were classified into different hazard classes based on their peak discharge values.

To assess the flash flood risk on the main outlet of wadi El-Alam Basin, where the town of Marsa Alam is located, the hydrological response (through the hydrographs) was required. To simulate such hydrographs, factors such as the duration, the size, and the location of the rainstorm have to be accommodated. The impact of these rainstorm characteristics upon the flooding event at the main basin's outlet is assessed by three sets of analyses. Firstly, it was assumed that the wadi was wholly covered by a 2-h rainstorm of varying rainfall depth (10–100 mm). Secondly, it is assumed that a rainstorm with a 2-h duration and 60-mm rainfall depth is exclusively covered a single sub-basin on each run of the model. Lastly, it is assumed that the basin was affected by a small rainstorm covering an area of only 5.5 km$^2$, which is usually the average size of a rainstorm in the arid regions (Sharon 1972).

## Results and discussion

### Hazard assessment for the Idfu-Alam highway

The 25 sub-basins (Fig. 6) that drain toward the Idfu-Alam highway were topographically diverse and varied in their physiographical characteristics giving them a differential effect on the highway. As shown from Table 1, the highest peak flows were mostly produced from sub-basins on the southern side of the Idfu-Alam highway together with a few on the northern side at the western end of the highway. The relatively large peak flows from the northern basins—such as sub-basins 19, 20, and 21—were found to be associated mainly with their high relief and main channel steep slope which help in reducing their flood lag times.

Since any flood damage is in direct relationship with its peak discharge and not with its total amount of discharge, the derived peak discharge values were used to classify the 25 sub-basins into four different hazardous categories (classes). As illustrated from Fig. 6, the first class is ranked as a low hazardous class and contains a group of 12 basins with a peak discharge of less than 5 m$^3$ s$^{-1}$. The second class is ranked as a moderately hazardous class and encompasses a group of ten basins with a peak discharge in the range of 5–20 m$^3$ s$^{-1}$. The third class is ranked as a highly hazardous class and includes one basin with a peak discharge in the range of 20–100 m$^3$ s$^{-1}$. The forth class is ranked as a very highly hazardous class and encompasses a group of two basins with a peak discharge of more than 100 m$^3$ s$^{-1}$.

In the flash flood event of 1991, two sites (among others) along the Idfu-Alam highway at 7 and 22.5 km, respectively, from the main basin's outlet were devastatingly damaged (El-Etr and Ashmawy 1993). The same two sites found to coincide exactly at the outlets of the two sub-basins of Id numbers 4 and 5, which were classified as very

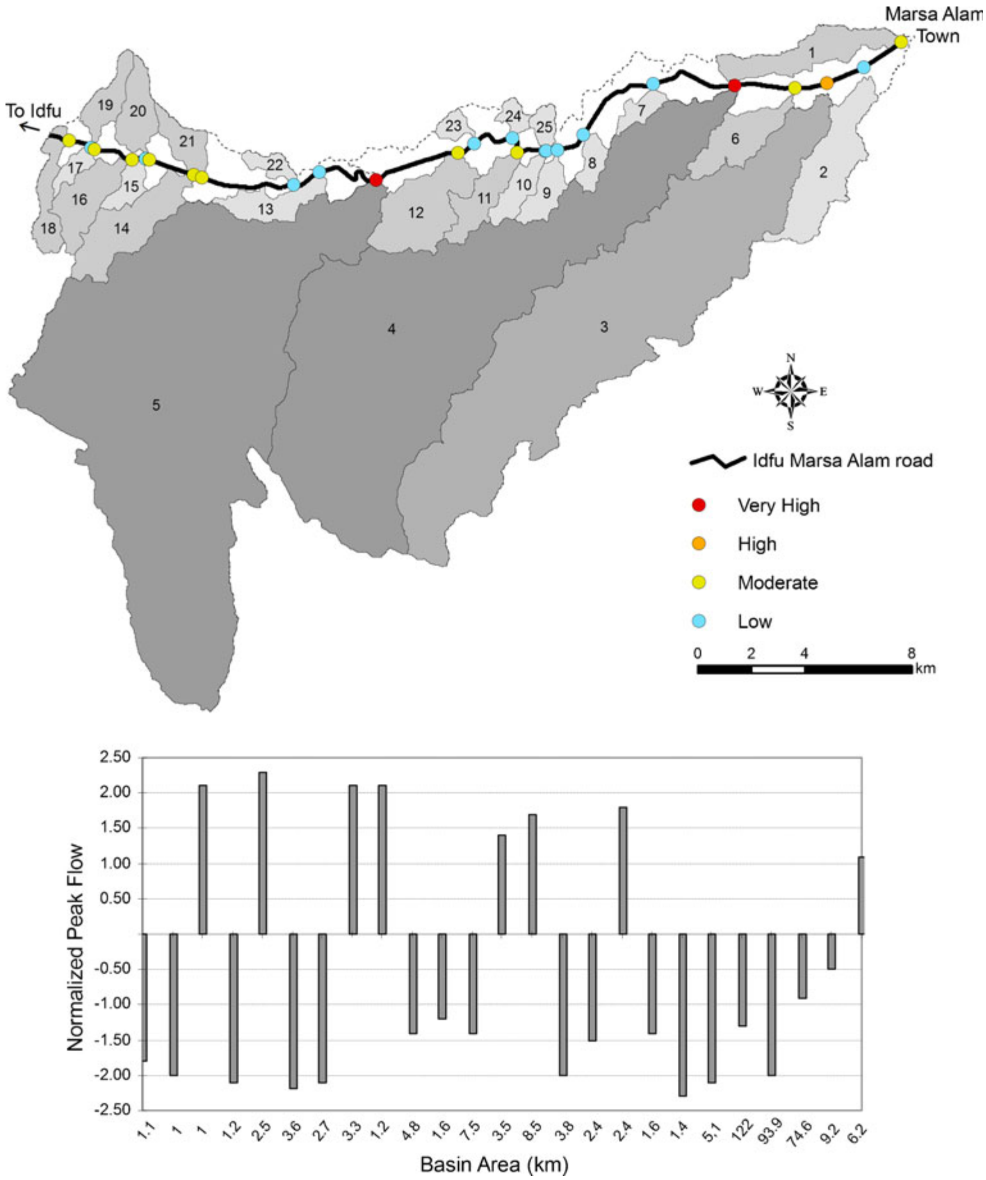


**Fig. 6** *Top* flash flood hazard map of Wadi El-Alam. The *shading* of the basins reflects the basin's hazard degree. The circle marks show both the location and level of hazard along the road. *Bottom* normalized peak flow of the 25 sub-basins of the El-Alam watershed

high hazard basins, thus indicating the reliability of the derived flood hazard map.

## Hazard assessment for the town of Marsa Alam

Visual inspection of the hazard map (Fig. 6) indicated that the hazardous sub-basins constituted a substantial amount of the total area of the El-Alam Basin and that they are the real sources of danger that threaten the highway not only at the points of their outlets but also at the very eastern end of the highway where the town of Marsa Alam is located. To assess the flood risk on the wadi outlet, where Marsa Alam is located, it was necessary to consider the dependence of the flood hazard upon factors such as the depth, the size, and the location of the rainstorm. So, here the extent of impact of the rainfall intensity on the basin hydrograph as well as the effect of the location of number of localized rainfall cells (covering different sites and different sub-basins) on the surface runoff behavior were investigated.

### *Assessment of the influence of rainfall depths on the runoff hydrograph*

In this section, the wadi has been assumed to be wholly covered by a 2-h rainstorm of varying rainfall depth (10–100 mm). The flood peak as a function of the rainfall is plotted in Fig. 7. From this figure, it is evident that for rainstorms of intensity ≤30 mm, surface storage absorbs the rainfall with a very little discharge at the basin mouth. With the increase of the rainfall intensity, the surface materials get saturated and the rate of infiltration decreases. For storms of intensity ≥40 mm, the rainfall

**Table 1** Morphometric parameters of the sub-basins of Wadi El-Alam draining toward the road

| Basin ID | Curve number | Average basin slope (%) | Main channel slope (%) | Area ($km^2$) | Peak flow ($m^3\ s^{-1}$) |
|---|---|---|---|---|---|
| 1 | 71.69 | 2.15 | 0.65 | 6.25 | 6.70 |
| 2 | 63.37 | 2.35 | 0.60 | 9.29 | 4.81 |
| 3 | 75.29 | 6.94 | 0.20 | 74.61 | 68.01 |
| 4 | 79.68 | 8.72 | 0.19 | 93.98 | 118.30 |
| 5 | 78.86 | 8.79 | 0.20 | 122.01 | 142.12 |
| 6 | 82.03 | 14.12 | 0.89 | 5.16 | 10.44 |
| 7 | 82.85 | 8.44 | 1.93 | 1.47 | 3.10 |
| 8 | 84.90 | 9.04 | 1.78 | 1.61 | 3.76 |
| 9 | 76.00 | 7.01 | 1.55 | 2.44 | 3.50 |
| 10 | 77.02 | 8.09 | 1.23 | 2.43 | 3.70 |
| 11 | 81.56 | 6.63 | 1.08 | 3.83 | 7.56 |
| 12 | 76.16 | 4.57 | 0.94 | 8.58 | 12.42 |
| 13 | 75.42 | 3.93 | 1.04 | 3.55 | 4.89 |
| 14 | 83.05 | 8.25 | 0.81 | 7.57 | 16.15 |
| 15 | 83.45 | 8.57 | 1.72 | 1.69 | 3.70 |
| 16 | 82.95 | 8.70 | 1.00 | 4.86 | 10.32 |
| 17 | 82.39 | 6.12 | 0.05 | 1.22 | 2.46 |
| 18 | 81.28 | 9.00 | 0.95 | 3.30 | 6.10 |
| 19 | 83.04 | 11.39 | 1.25 | 2.77 | 5.91 |
| 20 | 84.82 | 12.48 | 1.25 | 3.66 | 8.54 |
| 21 | 83.01 | 10.09 | 1.38 | 2.51 | 5.34 |
| 22 | 82.89 | 6.90 | 2.00 | 1.28 | 2.72 |
| 23 | 76.30 | 4.59 | 0.04 | 1.02 | 1.47 |
| 24 | 79.31 | 6.74 | 2.75 | 1.01 | 1.76 |
| 25 | 81.05 | 8.57 | 2.43 | 1.19 | 2.10 |

exceeds the ability of the surface to absorb the water. Thus, a surface runoff begins with a noticeable flood peak at the wadi's mouth. This surface runoff increases linearly with the rainfall intensity in accordance with the following equation:

$$\mathrm{FP} = 12.04(\mathrm{rd} - 40) + 127.50 \qquad \left(r^2 = 0.992\right); \qquad (2)$$

where FP is the flood peak (cubic meters per second) due to a rainfall of intensity rd (millimeters). The intercept of this relationship is the value of the flood peak at a rainfall of 40 mm at which a noticeable discharge sets in at the main basin's outlet. As wadi El-Alam is ungauged and there is very little meteorological data for the site, this equation might be useful for estimating the peak of any expected flood from just the precipitation intensity of rainstorm.

*Assessment of the influence of rainstorms covering different sub-basins on the runoff hydrograph*

Due to the nature of rainstorms in arid regions, which are typically characterized by localized convective cells (Sharon 1972; Zeller 1990; Blood and Humphrey 1990) that may cover only small area of the watershed, it is important to observe the shape of the hydrograph that results from rainstorms localized over different sub-basins of different sizes. Accordingly, the study basin was divided into six main sub-basins using the Strahler ordering approach. The flooding responses (hydrographs) of the sub-basins at the main outlet of the El-Alam Basin were computed for an assumed 2-h rainstorm of 60-mm rainfall depth exclusively covering just one sub-basin each time the HMS model was run.

Two observations were drawn from the computed hydrographs (Fig. 8). Firstly, the time to peak was influenced by the location of the sub-basin with respect to the main outlet of wadi El-Alam Basin. For example, the peak flow at the main wadi outlet, which resulted from a rainstorm over the Khariajah sub-basin (22 km away from the main outlet), appeared 1 h later than the peak flow resulted from a rainstorm over the Sukkari sub-basin (7 km away from the main outlet). Secondly, the start of the surface runoff of each sub-basin at the main outlet of the wadi El-Alam was not strongly dependent upon the location of the sub-basin. The explanation of these observations is

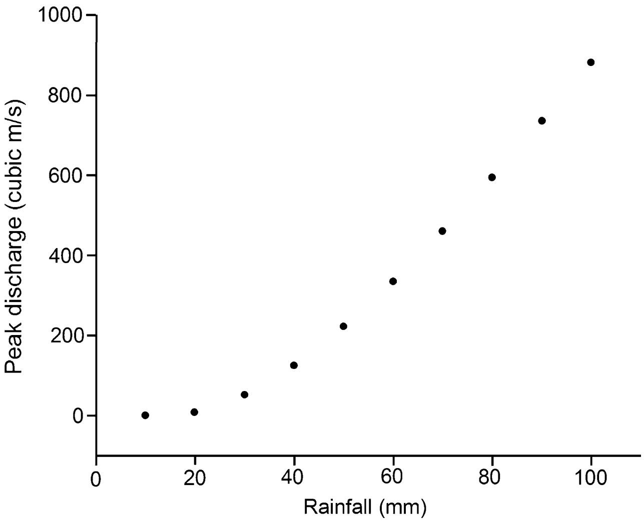


**Fig. 7** Flash flood peak of wadi El-Alam calculated at different rainfall depths

intricate, as more than one (compensating) variable comes into play. But the incipient appearance of the surface runoff within a narrow time slot at the main outlet might be explained by the permeability of the land cover, elevation, and location (distance) of the sub-basin. It is the compensating effect of the slope that makes the discharge of a distant sub-basin (such as wadi Kharijah) of low permeable surface initially appears, more or less at the same time as the discharge of a sub-basin of relatively high permeable surface and closer to the main outlet (such as wadi Alam). The relative shapes of the hydrographs might be explained in terms of the areas, shapes, and more importantly the locations of the sub-basins with respect to the main outlet.

*Assessment of the effect of rain cell location on the runoff hydrograph*

This section investigates the sensitivity of the wadi hydrological response to the spatial distribution of rainfall. To this end, five areas, each of 5.5 km$^2$, were specified at different locations over the basin under study. Each of these five areas was exclusively covered by a 2-h rainstorm of 60-mm rainfall depth. The HEC-HMS model was then used to calculate the time to peak and the peak discharge of the flood at the wadi mouth due to the applied rainstorm. It is apparent from the derived hydrographs (Fig. 9) that the location of the rainstorm had a major effect on the shape of the final hydrograph. The flood starts and hence peaks earlier if it is generated from a rainstorm located near to the main outlet. That is, the water of downstream flood has to travel shorter distance than that of the upstream one to reach the wadi mouth. Also, it has been noted that the upstream floods (e.g., site 4) are of a magnitude and a peak flows that are much higher than those for downstream ones (e.g., site 1). This might be attributable to the nature of the land cover, which is mainly coarse-grain deposits in the downstream areas (e.g., site 1) in contrast to the upstream ones, which is mostly composed of basement rocks and desert pavement of very low porosity (e.g., site 4).

To assess the impact of the rainfall depth, the precipitation intensity of the applied 2-h rainstorm was also varied for the five test areas to cover the range from 40 to 120 mm. Results show that the calculated flood peak varied linearly with the rainfall depth (Fig. 9b). For the five test sites under consideration, the standard deviation of the slope and intercept of their linear relationships are, respectively, 10% and 60% of the average. This indicates that the different sites respond more or less similarly to a certain rainfall event, but the actual flood peak that appears at the wadi mouth does differ in accordance with the location of the site. This brings up the question of what the average flood peak is at the wadi mouth regardless the location of the rain cell. The answer to this question lies in taking the average of the flood peak over different locations of the rain cell, which in turn the locations of the test sites. The least square fit of the average flood peak as a function of the rainfall depth is depicted in Fig. 10, with the individual response curve for each test site. This average flood peak is not only an average over the locations of the test sites but also is an average over their flood peak timings. If the number of the test sites is increased, ultimately one would end up with the whole basin covered with a rain cell of a projected surface area equals to that of the basin. Thus, the flood peak of the whole wadi El-Alam Basin (Eq. 2) normalized by its area (406.89 km$^2$) represents the morphometrical average of the flood peak

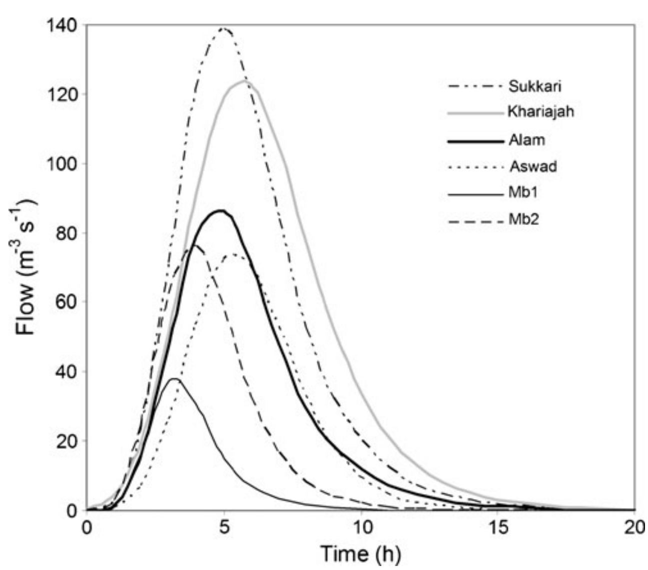


**Fig. 8** Hydrographs calculated at the outlet of wadi El-Alam for the six main sub-basins with the assumption that the rainstorm exclusively covers one sub-basin at a time

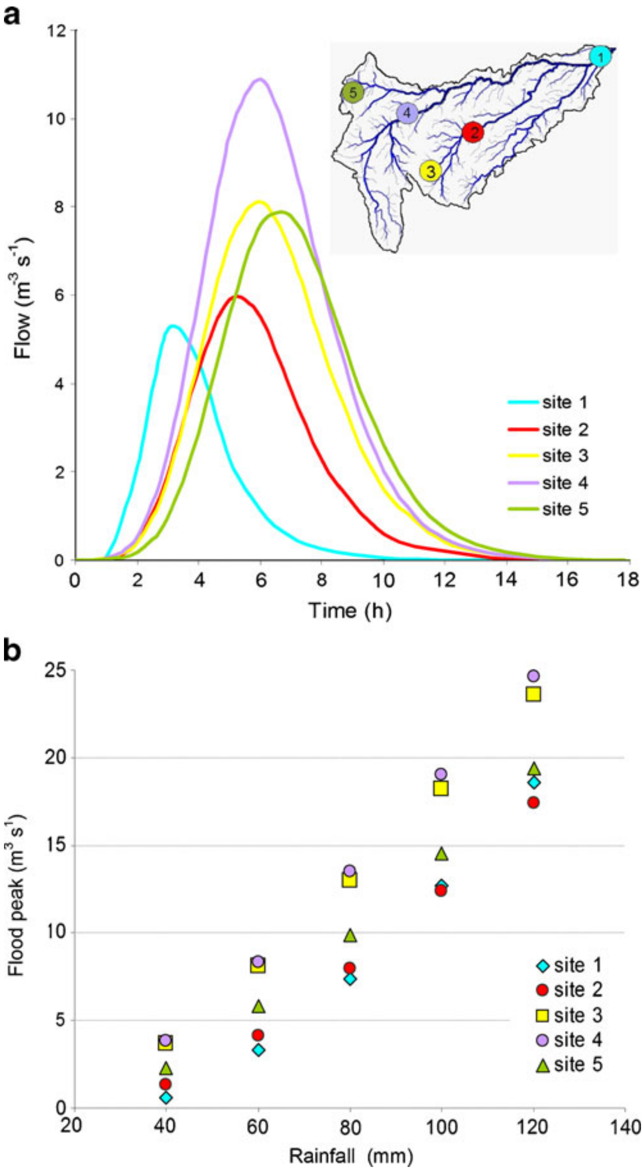


**Fig. 9** **a** Shows the derived hydrographs and **b** flow peaks of simulated 5.5 km$^2$ rain cells distributed over wadi El-Alam Basin

at its mouth due to a rain cell covering a unit area. Commonly, precipitation events in arid wadis such as wadi El-Alam are highly localized, with the rain cell covering only part of the wadi. Thus, for a given rain cell of precipitation intensity rd (millimeters) and covering an area rc (square kilometers), the average flood peak ($FP_{avg}$) at the main outlet of the wadi is given by the following equation:

$$FP_{avg}\left(m^3\ s^{-1}\right) = rc\ \times\ [0.03\ (rd - 40) + 0.313]\quad \text{for}\quad rd\ \geq\ 40\ \text{mm} \tag{3}$$

Given that the wadi is ungauged and there is no enough meteorological data for the site, this equation might be useful for predicting the response of the wadi to a precipitation event.

## Conclusions

Flash flood risk in arid regions is poorly understood and studied rarely due to a lack of data. Consequently, many infrastructure developments such as towns and roads are poorly located and unprotected from desert flood hazards. Here a modeling approach was used to predict flash flood hazard sites. The flood hazard was estimated not only on the basis of its location but also of the amount and timing of its discharge. This necessitates taking into account the excitation factor (rainfall) in the hydrological modeling approach used given the absence of the flooding records. This article has demonstrated that the hydrological response of the study basin to a rainfall is governed intrinsically by its geomorphometry and land cover types. Additionally, the response of the basin is very sensitive to the depth, the size, and the location of the rainstorm. Results demonstrate that wadi El-Alam Basin required a rainstorm intensity of at least 40 mm in order to initiate surface runoff with a noticeable flood peak at its main outlet. They also show that the location of rainstorm has a major effect on the shape of the basin final hydrograph. Moreover, in the study basin, the upstream flood appears to be of a magnitude and a peak flow that is much higher than those for downstream ones, which believes to be strongly attributed to the surface steepness and impermeability of the former.

In principle, the approach developed in the present study could be applied to any mountainous basins, in particular,

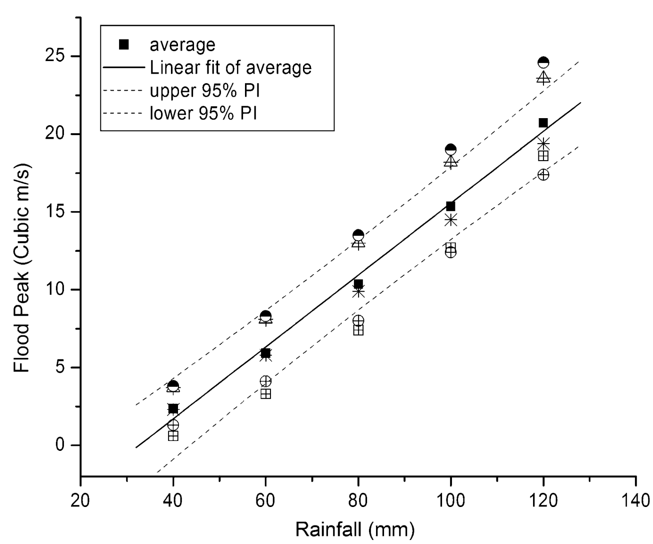


**Fig. 10** The least square linear fit of the calculated average flood peaks for five sites, each of area of 5.5 km$^2$, across wadi El-Alam Basin

those of the Eastern Desert and Sinai Peninsula in Egypt, which are similar to wadi El-Alam Basin in terms of their surface cover and terrain characteristics. These basins also often have settlements located near their outlets and may be traversed by roads in a similar fashion to that observed at wadi El-Alam. Moreover, as most of these basins are void of rainfall and flow gauges, an approach such as that presented in this article may be considered as a practical method for predicting flood hazards associated with such ungauged basins.

**Acknowledgments** The authors are greatly thankful to Nigel Arnell, Director of Walker Institute for Climate System Research, University of Reading, UK, for his comprehensive review and very useful comments.

## References

Al-Abed N, Abdulla F, Abu Khyarah A (2005) GIS-hydrological models for managing water resources in the Zarqa River basin. Environ Geol 47:405–411

Blood WH, Humphrey JH (1990) Design cloudburst and flash flood methodology for the western Mojave Desert, California. In: French RH (ed) Hydraulics/hydrology of aridlands ($H^2AL$). American Society of Civil Engineers, Reston, pp 561–566

Chow VT, Maidment DR, Mays LW (1988) Applied hydrology. McGraw-Hill, New York

Costa JE (1987) Hydraulics and basin morphometry of the largest flash floods in the conterminous United States. J Hydrol 93:313–338

El-Etr H, Ashmawy M (1993) Flash flood vulnerability and mitigation of the Red Sea basins between latitudes 24°41′ and 25°26′, Egypt. In: Proceedings of the International Conference 30 Years Cooper, Geological Survey of Egypt, Cairo, pp 335–351

Foody GM, Ghoneim EM, Arnell NW (2004) Predicting locations sensitive to flash flooding in an arid environment. J Hydrol 292:48–58

Gheith H, Sultan M (2002) Construction of a hydrologic model for estimating wadi runoff and groundwater recharge in the Eastern Desert, Egypt. J Hydrol 263:36–55

Ghoneim E (2008) Optimum groundwater locations in the northern Unites Arab Emirates. Int J Remote Sens 29(20):5879–5906

Ghoneim E, El-Baz F (2007) The application of radar topographic data to mapping of a mega-paleodrainage in the eastern Sahara. J Arid Environ 69:658–675

Ghoneim E, Robinson C, El-Baz F (2007) Relics of ancient drainage in the eastern Sahara revealed by Radar Topography data. Int J Remote Sens 28:1759–1772

Greenbaum N, Margalit A, Schick AB, Backer VR (1998) A high magnitude storm and flood in a hyperarid catchment, Nahal Zin, Negev Desert, Israel. Hydrol Process 12:1–23

Grodek T, Lekach J, Schick AP (2000) Urbanizing alluvial fans as flood-conveying and flood-reducing systems: lessons from the October 1997 Eilat flood. In: Hassan M, Slaymaker O, Berkowicz S (eds) The hydrology–geomorphology interface: rainfall, floods, sedimentation, land use. IAHS publication 261. IAHS, Wallingford, pp 229–250

Hammouri N, El-Naqa A (2007) Hydrological modeling of ungauged wadis in arid environments using GIS: a case study of Wadi Madoneh in Jordan. Revista Mexicana de Ciencias Geológicas 24 (2):185–196

Jenson SK, Domingue JO (1988) Extracting topographic structure from digital elevation model data for geographic information system analysis. Photogramm Eng Remote Sens 54:1593–1600

Patton PC (1988) Drainage basin morphometry and floods. In: Baker VR, Kochel RC, Patton PC (eds) Flood geomorphology. Wiley, New York, p 503

Patton PC, Baker VR (1976) Morphometry and floods in small basins subject to diverse hydro-geomorphic controls. Water Res Res 12:941–952

Peters JC (1998) HEC-HMS, hydrologic modeling system. US Army Corps of Engineers, Hydrologic Engineering Center, Davis

Philip JR (1957) The theory of infiltration: 4. Sorptivity and algebraic infiltration equations. Soil Sci 84:257–264

Reid I, Laronne JB, Powell MD (1998) Flash-flood and bedload dynamics of desert gravel-bed streams. Hydrol Process 12:543–557

Schick AP, Grodek T, Lekach J (1997) Sediment management and flood protection of desert towns: effect of small catchments. In: Walling DE, Probst JL (eds) Human impact on erosion and sedimentation. IAHS publication 245. IAHS, Wallingford, pp 183–189

SCS (1985) National engineering handbook. US Department Agriculture, Soil Conservation Service, Washington, DC

Sharon D (1972) The spottiness of rainfall in a desert area. J Hydrol 17:161–175

Sorman AU, Abdulrazzak MJ, Elhames AS (1990) Rainfall–runoff modeling of a microcatchments in the western region of Saudi Arabia. In: Lang H, Musy A (eds) Hydrology in mountainous regions: hydrological measurements, the water cycle. IAHS publication 193. IAHS, Wallingford, pp 655–659

Tso B, Mather PM (2001) Classification methods for remotely sensed data. Taylor and Francis, London

Zeller ME (1990) Precipitation on arid or semiarid regions of the southwestern United States: research needs from a consultant's perspective. In: French RH (ed) Hydraulics/hydrology of arid lands ($H^2AL$). American Society of Civil Engineers, Reston, pp 525–529